Applied Energy 132 (2014) 325–338

Contents lists available at ScienceDirect

Applied Energy

journal homepage: www.elsevier.com/locate/apenergy

A Multi-Approach Evaluation System (MA-ES) of Organic Rankine Cycles (ORC) used in waste heat utilization

Gequn Shu, Guopeng Yu, Hua Tian *, Haiqiao Wei, Xingyu Liang

State Key Laboratory of Engines, Tianjin University, 92 Weijin Road, Nankai District, Tianjin 300072, China

HIGHLIGHTS

- The MA-ES provides comprehensive valuations on ORC used for waste heat utilization.
- The MA-ES covers energetic, exergetic and economic evaluations of typical ORCs.
- The MA-ES is a general assessing method without restriction to specific ORC condition.
- Two ORC cases of ICE waste-heat-recovery are exemplified applying the MA-ES.

ARTICLE INFO

Article history:
Received 21 November 2013
Received in revised form 22 May 2014
Accepted 4 July 2014
Available online 31 July 2014

Keywords:
Multi-Approach Evaluation System (MA-ES)
Organic Rankine Cycles (ORC)
Waste heat utilization
Modeling

ABSTRACT

A Multi-Approach Evaluation System (MA-ES) is established in this paper providing comprehensive evaluations on Organic Rankine Cycles (ORC) used for waste heat utilization. The MA-ES covers three main aspects of typical ORC performance: basic evaluations of energy distribution and system efficiency based on the 1st law of thermodynamics; evaluations of exergy distribution and exergy efficiency based on the 2nd law of thermodynamics; economic evaluations based on calculations of equipment capacity, investment and cost recovery. The MA-ES is reasonably organized aiming at providing a general method of ORC performance assessment, without restrictions to system configurations, operation modes, applications, working fluid types, equipment conditions, process parameters and so on. Two ORC cases of internal combustion engines' (ICEs) waste-heat-recovery are exemplified to illustrate the applications of the evaluation system. The results clearly revealed the performance comparisons among ORC configurations and working fluids referred. The comparisons will provide credible guidance for ORC design, equipment selection and system construction.

1. Introduction

The issue of global energy inadequacy, together with climate and economic issues, has become more and more urgent currently. Countries around the world are developing policies and techniques in industries for better utilization of residual energy that accounts a great part of original fuel energy. Residual energy in industries mainly refer to low and medium grade waste heat, which accounts for more than half of the total heat generated [1], and it widely exists in almost every industrial field, especially in cement industry, oil industry, engines, gas turbines, solar field, biomass and geothermal fields [2,3].

Among various techniques of utilizing residual energy, Organic Rankine Cycle (ORC) is receiving more and more attention for its high efficiency and flexibility, and good matching between working fluids and low and medium grade heat sources. Comparing with steam rankine cycle (RC) under the same residual conditions, ORC has the advantages of higher thermal efficiency, more net power, smaller system volume and weight as well as less complex expander devices, etc. [4]. It can be concluded from literature survey that plenty of theoretical researches on ORC systems used in low and medium grade heat utilization have been conducted focusing on various applications, working fluid types [5,6], operation modes [27], system configurations [28], specific components [7] and performance parameters. Actually, a reasonable and comprehensive evaluation system is essential to ORC systems used in waste heat utilization to provide guiding assessments and comparisons of different ORC operations. Among current evaluation researches, three main analysis aspects of ORC performance are

* Corresponding author. Postal address: State key laboratory of engines, Tianjin University, 92 Weijin Road, Nankai District, Tianjin 300072, China. Tel./fax: +86 22 27409558.
E-mail address: thtju@tju.edu.cn (H. Tian).

http://dx.doi.org/10.1016/j.apenergy.2014.07.007
0306-2619/

Nomenclature

Abbreviations

ORC	Organic Rankine Cycle
MA-ES	Multi-Approach Evaluation System
BSFC	brake specific fuel consumption
CHP	combined heating and power system
EIP	expander-inlet-pressure [MPa]
PPTD	Pinch Point Temperature Difference method
HTC	heat transfer coefficient [W/(m^2 K)]
tHTC	Total heat transfer coefficient [kW/(m^2 K)]
CEPCI	Chemical Engineering Plant Cost Index
CRF	capital recovery factor
EPC	the electricity production cost [Dollar/kW h]
DPP	depreciated payback period
NPV	net present value
SL	the single-loop ORC
DL	the dual-loop ORC
HL	the high-temperature loop of DL ORC
LL	the low-temperature loop of DL ORC

Symbols

P	power [kW]
Q	heat flow [kW]
E	exergy flow [kW]
I	exergy loss [kW]
T	temperature [K]
$\dot{m}$	mass flow rate [kg/s]
cp	specific heat capacity [kJ/(kg K)]
t	plate thickness [m]
λ	coefficient of thermal conductivity [kW/(m K)]
η	efficiency [dimensionless]
α	heat transfer coefficient [W/(m^2 K)]
β	chevron angle [degree]
ρ	density of working fluid [kg/m^3]
μ	viscosity [pa s]
v	velocity [m/s]
h	specific enthalpy [kJ/kg]
s	specific entropy [kJ/(kg K)]
f_g	the friction factor in exhaust gas side
Re	Reynolds number [dimensionless]
Pr	Prandtl number [dimensionless]
Nu	Nusselt number [dimensionless]
G	working fluid mass flux [kg/m^2 s]
g	acceleration due to gravity [m/s^2]
i_{fg}	the enthalpy of vaporization [kJ/kg].
Fr	Froude number [dimensionless]
Co	convection number[dimensionless]
Bo	boiling number [dimensionless]
x	the vapor quality
Deq	the equivalent diameter of working fluid channel
p_{cr}	the critical pressure of working fluid [MPa]
$p_e/p_{\max}$	the evaporating pressure of working fluid; EIP; the maximum pressure of the ORC cycle[MPa]
R_p	mean asperity height [μm]
q	the heat flux [W/m^2]
M	molar mass of working fluid [kg/kmol].
K	tHTC; the total heat transfer coefficient of a heat exchanger [kW/(m^2 K)]
A	heat transfer area [m^2]
A_s	heat transfer area per net power [m^2/kW]
ΔT_m	logarithmic mean temperature difference
A_{nk}	annuity of the investment [Dollar]
f_K	the maintenance and insurance cost factor

Superscripts and subscripts

0	dead state
system	the whole ORC system
1st	the first law of thermodynamics
2nd	the second law of thermodynamics
hs	the heat source
cs	the cold source
f	the working fluid
hsf	the process between the heat source and working fluid
gf	the process between the exhaust gas and working fluid
fcw	the process between the working fluid and cooling water
pp	the pinch point
g	the exhaust gas
jw	the jacket water
cw/*c*/*condens*	the cooling water for condensing; the condensing process
v	the vapor state
l	the liquid state
wall/*w*	the wall-temperature state
e/*evp*	the evaporation process
bm	the bare module
exp	the expander
fp/*pump*	the working fluid pump
pre	the preheated region of working fluid
suph	the superheated region of working fluid
supc	the superheated region of working fluid in the condensing process (5–6)
cond	the condenser/condensation
cout	the cooling water flowed out from the condenser
*f*1*f*2	the process between the two working fluids of two loops in DL ORC
*jwf*2	the process between the jacket water and working fluid in the low-temperature loop of the DL ORC
*f*1,exp1,η_1,*g*1,*gf*1,*pump*1	parameters or processes of the high-temperature loop of the DL ORC
*f*2,exp2,η_2,*g*2,*gf*2,*pump*2,*supc*2,*cond*2	parameters or processes of the low-temperature loop of the DL ORC
1-13,2*g*,3*g*,5*s*,7*s*,13*s*	state points

generally considered, i.e., basic energy aspect, exergy aspect and economical aspect.

As to the basic energy analyses of ORC systems, Iacopo and Agostino [8] described a specific thermodynamic analysis in order to efficiently match ORC system with stationary internal combustion engine (ICE). Main target parameters concerned consisted of the ORC efficiency, net power output, mass flow rate of working fluid, and turbine outlet/inlet volume flow ratio, etc. The investigations were mainly based on the basic energy analyses of ORC systems by manipulating turbine inlet pressure. Katsanos et al. [9] conducted a theoretical study to investigate the potential improvement of the overall efficiency of a heavy-duty truck diesel engine equipped with an ORC bottoming system for recovering heat from exhaust gas. Based on basic energy level analysis, main target parameters concerned are brake specific fuel consumption (BSFC) improvement of diesel, ORC generated power, working fluid mass flow rate, cycle high pressure and cycle efficiency. Zhang et al. [10] proposed a novel system combining a vehicular light-duty diesel engine with a dual

loop ORC, which recovers waste heat from the engine exhaust, intake air and coolant. Main target parameters include the overall net power, thermal efficiency, improvement of engine effective power and improvement of BSFC by manipulating the engine conditions, namely, the heat sources' conditions. Lisa et al. [11] analyzed and compared various possible modifications to simple ORC plant layout, such as recuperated cycles, superheated cycles, supercritical cycles, regenerative cycles and their combinations. Based on basic energy assessments, six main thermodynamic indexes were investigated, including cycle efficiency, specific work, recovery efficiency, turbine volumetric expansion ratio, ORC fluid-to-hot source mass flow ratio and heat exchangers size parameter. The investigations were aimed at providing useful guidelines for selecting ORC configuration, appropriate fluids and for defining operating parameters with specific given application.

As to the exergy analyses of ORC systems, Huijuan et al. [12] researched on transcritical Rankine cycles using refrigerant R32 (CH_2F_2) and carbon dioxide (CO_2) as the working fluids for the conversion of low-grade heat into mechanical power. Aside from basic energy calculations, analysis of the exergy destruction and loss as well as the exergy efficiency optimization of transcritical Rankine cycle was conducted. Yiping et al. [13] optimized the thermodynamic performance of ORCs for waste heat recovery with exergy efficiency as an objective function by means of genetic algorithm. One result showed that the ORC system using R236ea has higher exergy efficiency than other working fluids did under the same condition of given waste heat. Roy et al. [14] developed a computer program to parametrically optimize and compare the systems and second law efficiency, irreversibility of the system, availability ratio, work output and mass flow rate with increasing turbine inlet temperature of ORC under different conditions of heat source. They confirmed that a non-regenerative ORC during superheating using R123 appears to be a good choice for converting low-grade heat to power with high efficiencies, turbine work output and low irreversibility. Tchanche et al. [15] studied on three modified engines derived from simple Rankine engine using regeneration (incorporation of regenerator or feed-liquid heaters) with exergy-topological method. Exergy destruction throughout the systems operating with R134a was quantified and illustrated using exergy diagrams. The results revealed that greater exergy destruction occurred in devices such as turbine, evaporator and feed-liquid heaters than in other devices. Similar exergy analyses of ORC systems were conducted in Refs. [16–18].

As to the economical analyses of ORC systems, Hua et al. [4] proposed an ORC model used to recover waste heat in ICE exhaust gas. The ORC system was techno-economically analyzed. The screening criteria included the thermal efficiency of ORC, expansion ratio, net power output per unit mass flow rate of hot exhaust, the ratio of total heat transfer area to net power output and electricity production cost. Lecompte et al. [19] developed a thermo-economic calculation procedure for ORC taking into account of part load operations. The methodology was applied to a CHP system driven by an ICE where waste heat is available from the closed loop engine cooling circuit. The economically optimal ORC system was firstly sized for the heat source and then was used in an hour-by-hour quasi-steady state simulation over a reference year to investigate possible net energy productions. Schuster et al. [20] developed energetic and economic investigations of ORC systems used in various applications. It revealed that the efficiency of waste-heat-recovery utility is strongly dependent on the interest rate and the full load hours of the system and that reliable and long operation is necessary for an economic operation of a waste-heat-recovery unit. The thermodynamic and economic performance of both subcritical and transcritical ORC systems were examined for low-temperature geothermal power plant by Shengjun et al. [21]. They conducted a simulation procedure using five indicators: thermal efficiency, exergy efficiency, recovery efficiency, heat exchanger area per unit power output and levelized energy cost. The saved petroleum and reduced CO_2 emission per year were also simply estimated. Gewald et al. [22] explored rankine cycles as bottoming waste-heat-recovery cycles to enhance electrical efficiency of internal combustion engines. Energetic, exergetic and economic analyses were conducted. The annuities of capital-related and operation-related costs as well as the specific costs of electricity production were calculated. Pedro and Rogelio [23] have presented a simple methodology to determine the economic, energetic and environmental potential benefits that can be obtained from the implementation of an MT-ORC. Economic indexes like operational cost, primary energy consumption savings and payback period have been investigated.

Previous ORC researches as reviewed above are mostly not comprehensive enough to cover all important aspects of system performance. Although each of the three ways of evaluations has been proposed and applied to varying degrees by other researchers in many chemical engineering fields, it is of great importance to select, combine and complement the evaluations in order to form a comprehensive system for ORC evaluation.

In this work, a comprehensive evaluation system of ORC performance, which is defined as a Multi-Approach Evaluation System (MA-ES), is established in this paper by combining and complementing the existing ORC modeling methods. Based on the MA-ES, theoretical analyses and performance comparisons of ORC systems will become more comprehensive and clear, since it provides a general method of ORC performance assessment, without restrictions to system configurations, operation modes, applications, working fluid types, equipment conditions and process parameters, etc. The comparisons will provide valuable guidance for ORC design, equipment selection and system construction. Finally, two typical ORC cases of engine waste-heat-recovery are investigated in this work to illustrate the applications of the evaluation system.

2. MA-ES descriptions

The proposed MA-ES comprises three main parts covering the aspects of ORC performance. They are illustrated in the schematic diagram in Fig. 1 and are explained in detail as follows one by one.

Way1 of the MA-ES focuses on evaluations based on the 1st law of thermodynamics, i.e., energy conservation principle. The aim of this part is to investigate the energy distributions and conversions in quantity level. It is the fundamental part for ORC researches and is essential for further investigations. The most typical performance indexes in this part include net power P_{net} and system efficiency η_{1st} (the 1st law efficiency), etc. The detailed modeling is presented in Section 3.2.

Way2 of the MA-ES focuses on evaluations based on the 2nd law of thermodynamics, which is to probe into the exergy distributions of ORC systems. Basic computations based on heat balance in Way1 cannot reflect explicitly the extent of energy utilization. Evaluations of system exergy are indispensible since on the one hand, they can figure out how efficient the energy is converted and utilized in quality level and on the other hand, they can reveal the exergy losses occurred in each component and find out the component with the maximum exergy loss, pointing out optimizing directions. The typical performance indexes in this part include total exergy loss I^{system} and exergy efficiency η_{2nd} (the 2nd law efficiency), etc. The detailed modeling is presented in Section 3.3.

Way 3 of the MA-ES focuses on techno-economic evaluations of ORC systems based on calculations of components' capacity, investment and cost recovery. This part is significant for comprehensive evaluations on ORC system and is meaningful for system

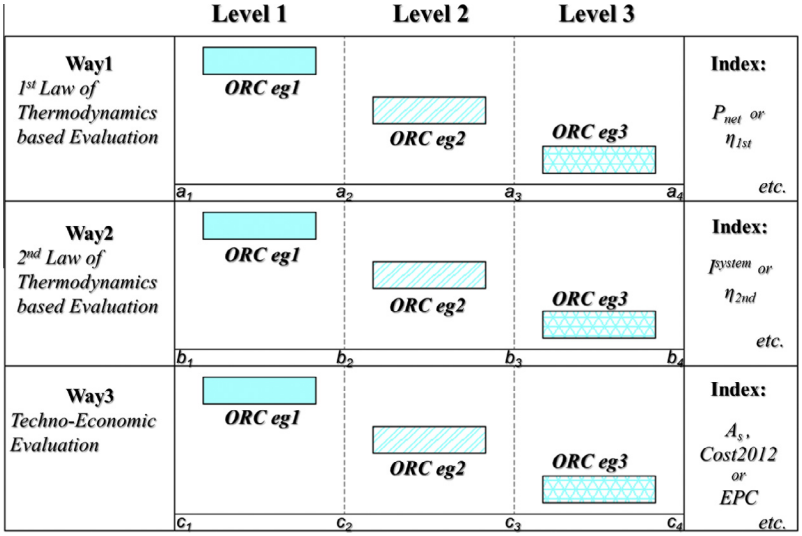

Fig. 1. Schematic diagram of the ORC Multi-Approach Evaluation System (MA-ES).

design and construction by providing credible predictions and guidance. Many costs other than purchased costs of equipments are taken into consideration in the economic evaluations of an integrated ORC system. The factors associated with system investments include direct project expenses, indirect project expenses, contingent and contractor fees as well as auxiliary facility expenses. In addition, material factors and pressure factors are taken into account in the cost evaluations. Associating with thermodynamic calculations in the first two ways, the amount of investment and cost recovery period can be figured out by the techno-economic evaluations in this part. The detailed modeling is presented in Section 3.4.

As shown in the schematic diagram of Fig. 1, three fictitious examples of ORC system (ORCeg1, ORCeg2, ORCeg3) are proposed to better interpret the evaluation system. Hypothetically, they are three different systems running under the same given boundary condition. Evaluation results are collected in Fig. 1 to compare their performance. Comparing the three sets of result, the value range of each index can be easily got. The value ranges of all indexes are graded into three levels (like Level 1: a_1–a_2, Level 2: a_2–a_3, Level 3: a_3–a_4) averagely and increasingly in order to precisely reveal the relative performance of each system. According to the 1st law of thermodynamics based analysis in the Way1 part, the ORCeg1 system performs poorly with low P_{net} or η_{1st} which are ranked in Level1 while the ORCeg3 performs the opposite. According to the 2nd law of thermodynamics based analysis in the Way2 part, the I^{system} of ORCeg1 is the lowest which means the least exergy loss. However, if the η_{2nd} is chosen as the representing index in this part, the ORCeg1 shows the biggest irreversibility with the lowest η_{2nd}.

Meanwhile, the low level (Level 1) in Way 3 evaluation is the low-cost and good-economy region. As shown in this example, economical indexes of ORCeg1 obtained from Way 3 evaluations are all lower than those of the other two systems, meaning better economic performance. The ORCeg3 system indicates opposite characteristics with the largest economic indexes. Overall, the ORCeg2 is a medium system with moderate performance.

The evaluation system operates in this way for clearly revealing of ORC system performance. It is modeled and expounded in detail in the paragraphs below.

3. MA-ES modeling and analyzing

The MA-ES modeling process in this part is introduced based on a conventional ORC system. A basic ORC system could derive kinds of ORC modifications, such as preheated ORCs [8,24], regenerative ORCs [11,25] and dual-loop ORCs [10,25,26]. By making corresponding adjustments to specific correlations and coefficients, the proposed MA-ES is applicable to all ORC modified configurations because they originate from the same ORC principle. It provides a general method of ORC performance assessment, without restrictions to system configurations, operation modes, applications, working fluid types, equipment conditions and operation parameters, etc.

3.1. ORC descriptions

The basic ORC principle is illustrated in Figs. 2–4. In a word, a complete ORC system basically comprises a compressing process in the pump for pressure lifting, a heating process by hot sources for temperature increasing, an expanding process in the expander for power output and a condensing process in the condenser for fluid cooling down. Cycles run continuously in this way to generate continuous power. ORC operations are typically divided into two operating modes by expander-inlet-pressure (EIP). They are subcritical systems with EIP below critical pressure and transcritical systems with EIP above critical pressure [27], as shown in Figs. 3 and 4 separately.

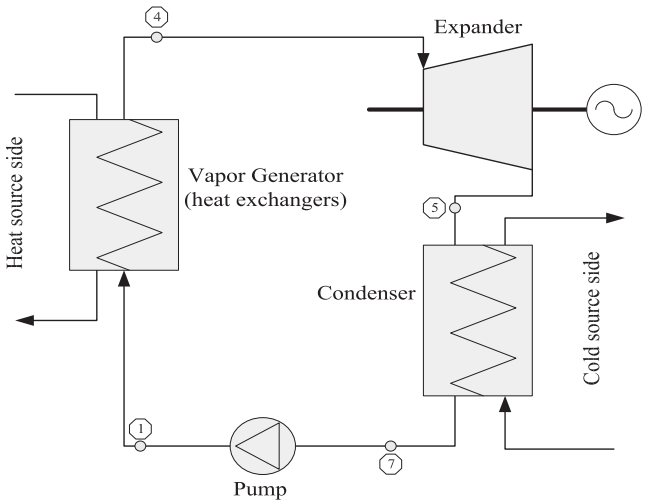

Fig. 2. Schematic diagram of a typical ORC system.

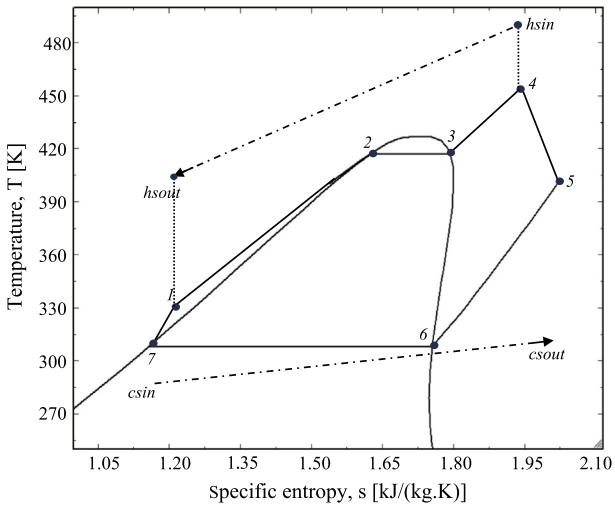

Fig. 3. T–S diagram of a typical subcritical ORC system.

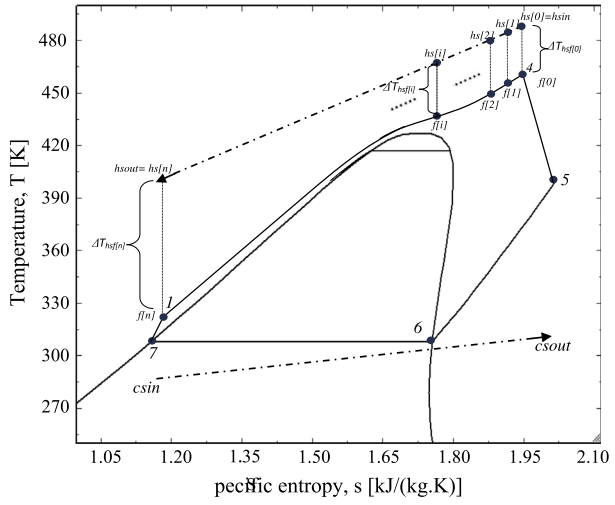

Fig. 4. T–S diagram of a typical transcritical ORC system applying PPDT method.

Before establishing the MA-ES models, assumptions are made as following: each component is considered as a steady-state and steady-flow system; the kinetic and potential energies as well as heat and friction losses are neglected; the isentropic efficiencies of the pump and the expander are set at constant values. Besides, boundary conditions for simulations should be set clearly according to certain ORC applications, including environmental conditions, isentropic efficiencies of the pump and the expander, heat and cold source conditions, crucial operating parameters, pinch temperatures of heat exchangers, and so on.

3.2. MA-ES Way1: The 1st law of thermodynamics analysis

Way1 shows the first way of performance evaluating based on energy level analysis. In this part, the energy balance equations of system components and the system efficiency equation are listed in the second column in Table 1. It can be revealed that, the energy conversion in each component is an arithmetic product of the mass flow rate of working fluid and the enthalpy difference of inlet and outlet fluid. So the fundamental calculation target in this part is the mass flow rate of the working fluid, which determines the thermodynamic state of every point in the ORC system and the performance of the whole system. A common method for mass flow rate calculation and thermodynamic states' computation is the Pinch Point Temperature Difference (PPTD) method [4,8]. The PPTD method was illustrated for subcritical ORC in previous work by Tian of our group [4]. In this work, the method is further introduced for transcritical system since the modeling process is quite different in the two system modes.

Take the transcritical cycle in Fig. 4 for instance, the heat exchange between the heat source and working fluid can be evaluated as following by applying PPTD method. Parameters like the temperature of the inlet heat source T_{hsin}, mass flow rate of heat source $\dot{m}_{hs}$, working fluid temperatures at point 1 and point 4 have been known prior to this calculation. The pinch point temperature of this heat exchange process is expected to be T_{pp}.

Step 1, the temperature of the outlet heat source is assumed as T_{hsout} (a constant value), thus the temperature difference (ΔT_{hs}) of the inlet and outlet heat sources is got.

Step 2, the mass flow rate of working fluid ($\dot{m}_{f0}$) can be preliminarily determined by the following Eq. (1).

$$\dot{m}_{f0} = \frac{cp_{hs}\dot{m}_{hs}(T_{hsin} - T_{hsout})}{cp_f(T_4 - T_1)} \tag{1}$$

Step 3, the temperature difference (ΔT_{hs}) of the heat source is evenly divided into N (N is a constant value) segments from $T_{hs[0]}$ to $T_{hs[n]}$. Namely, T_{hsin} is equal to $T_{hs[0]}$, and T_{hsout} is equal to $T_{hs[n]}$. Correspondingly, the heating process of working fluid from point 1 to point 4 is divided evenly from $T_{f[0]}$ to $T_{f[n]}$, and T_4 is equal to $T_{f[0]}$, T_1 is equal to $T_{f[n]}$. Besides, $T_{hs[i]}$ reflects a random point between the inlet and outlet heat sources. The step-length is set to be Δ,

$$T_{hs[1]} = T_{hs[0]} - \Delta \tag{2}$$

Step 4, the working fluid temperature at point f_1 ($T_{f[1]}$) will be acquired easily based on heat balance with known parameters $T_{hs[0]}$, $T_{hs[1]}$, $\dot{m}_{hs}$, T_4 and $\dot{m}_{f0}$, and the temperature difference between heat source and working fluid in the first segment is acquired as

$$\Delta T_{hsf[1]} = T_{hs[1]} - T_{f[1]} \tag{3}$$

Similarly, calculations are conducted gradually in all the N segments, and the temperature differences at any points ($\Delta T_{hsf[i]}$) can be obtained.

Table 1
Thermodynamic models used in Way1 and Way2 evaluations of MA-ES.

	Energy distributions	Exergy losses distributions
Expander	$P_{expander} = \dot{m}_f \cdot (h_4 - h_5)$	$I_{expander} = \dot{m}_f \cdot (s_5 - s_4) \cdot T_0$
Work fluid pump	$P_{pump} = \dot{m}_f \cdot (h_1 - h_7)$	$I_{pump} = \dot{m}_f \cdot (s_1 - s_7) \cdot T_0$
Evaporator/heater	$Q_{heat} = \dot{m}_f \cdot (h_4 - h_1)$ or $Q_{hs} = cp_{hs} \cdot \dot{m}_{hs} \cdot (T_{hsin} - T_{hsout})$	$I_{heat} = (E_{gin} + E_1) - (E_{gout} + E_4)$
Condenser	$Q_{condens} = \dot{m}_f \cdot (h_5 - h_7)$ Or $Q_{condens} = cp_{cw} \cdot \dot{m}_{cw} \cdot (h_{cout} - h_{cin})$	$I_{condens} = (E_{cwin} + E_5) - (E_{cwout} + E_7)$ And $I_{out}^{cold\text{-}source} = E_{cwout} - E_{cwin}$
System	$P_{net} = P_{expander} - P_{pump}$	$P_{net} = E_{in}^{hot\text{-}source} - I^{system}$
Efficiency	$\eta_{1st} = P_{net}/Q_a \cdot 100\%$	$\eta_{2nd} = P_{net}/E_{in}^{hot\text{-}source} * 100\%$

Step 5, the minimum temperature difference can now be known as ΔT_{hsf_min} by comparing all the calculated temperature differences from $\Delta T_{hsf[1]}$ to $\Delta T_{hsf[n]}$ ($N+1$ values). Comparing the $\Delta T_{hsf\text{-}min}$ and the expected value T_{pp}. If the deviation is acceptable, it means the assumed value of T_{hsout} in Step 1 is reasonable. Otherwise, the value of T_{hsout} should be modified to a new one. The calculation is then needed to be repeated from step 1 to step 4 until a satisfactory deviation occurs. During the last iteration, the mass flow rate $\dot{m}_f$ and outlet temperature of heat source T_{hsout} are successfully determined. The state parameters of each point as well as energy distributions and efficiencies are then obtained according to Table 1.

3.3. MA-ES Way2: The 2nd law of thermodynamics analysis

Way2 shows the second way to evaluate the system performance based on exergy level analysis [29]. In this part, the system's exergy performance can be evaluated as following.

As to the whole system, the exergy balance equation and exergy destruction equation are defined as,

$$E_{in}^{hot\text{-}source} + P_{pump} = P_{expander} + I^{system} \tag{4}$$

$$I^{system} = I_{out}^{cold\text{-}source} + I_{heat\text{-}exchangers} + I_{pump} + I_{expander} \tag{5}$$

$E_{in}^{hot\text{-}source}$ is the net input exergy from the heat source. P_{pump} and $P_{expander}$ are the pump power and expander power respectively. I^{system} is the system's total exergy loss, containing the exergy lost away with outlet cold source ($I_{out}^{cold\text{-}source}$), the exergy losses resulted from non-isentropic compression and expansion (I_{pump} and $I_{expander}$), and the exergy lost during all heat transfer processes ($I_{heat\text{-}exchangers}$). The $I_{heat\text{-}exchangers}$ contains exergy lost in the vapor generator (I_{heat}) and the condenser ($I_{condens}$). Specific equations of each process are listed in the third column of Table 1.

3.4. MA-ES Way3: The techno-economic analysis

Way3 shows the third way to evaluate the system performance focusing on economic analysis. The work in this part is mainly referred from the book [30], which is widely used for analysis, synthesis and design of chemical processes. The capacities of the expander and the pump refer to the expansion power $P_{expander}$ and the pump power consumptions P_{pump}, which have been obtained from Way1 evaluation. The capacity of a heat exchanger refers to its heat transfer area, which is the first main target in the part of economic evaluation.

3.4.1. Calculations of heat exchangers' capacities

The calculation process of heat transfer area includes three steps as described below.

Step1, choose proper types of heat exchangers according to applications. As to different fluid types under different thermodynamic conditions, heat exchangers should be carefully selected for the best heat transferring and easiest construction. Whichever type of heat exchanger is chosen, the calculation process is similar as introduced below. Plate heat exchangers are chosen here for instance, based on the products bought in our research group. The plate heat exchangers are popular in modern power and process industries due to its advantages and outstanding capability to recover heat with extremely small temperature difference, etc. [31,32].

Step 2, choose proper heat transfer correlations. Various kinds of heat transfer correlations have been studied and published according to different applications. None of them is identified as the best one for all applications. Proper selections of heat transfer correlations are essential to creditable evaluation about the aimed capacity. The correlations below are selected for the basic ORC example mentioned in Figs. 2–4. Besides, the hot source is supposed to be exhaust gas from industry, and the cold source is domestic water.

The hot exhaust gas is supposed to stay in single phase, and its heat transfer coefficient (HTC) α_g is obtained by the following equations [33]. The correlation proposed by Gnielinski takes additionally the effect of wall roughness into account by means of the friction factor f_g.

$$f_g = (1.82 \cdot \lg \mathrm{Re}_g - 1.5)^{-2} \tag{6}$$

When $\mathrm{Re}_g > 10^4$ and $\mathrm{Re}_g < 5 \times 10^6$,

$$\mathrm{Nu}_g = (f_g/8) \cdot (\mathrm{Re}_g - 1000) \cdot \mathrm{Pr}_g / [12.7 \cdot (f_g/8)^{0.5} \cdot (\mathrm{Pr}_g^{2/3} - 1) + 1.07] \tag{7}$$

When $\mathrm{Re}_g < 10^4$,

$$\mathrm{Nu}_g = (f_g/8) \cdot \mathrm{Re}_g \cdot \mathrm{Pr}_g / [12.7 \cdot (f_g/8)^{0.5} \cdot (\mathrm{Pr}_g^{2/3} - 1) + 1.07] \tag{8}$$

$$\alpha_g = Nu_g \cdot k_g / D_{eq,g} \tag{9}$$

Wherein, f_g is the friction factor, and the subscript g means the hot exhaust gas.

Correlations chosen for subcritical systems (Fig. 3) are firstly introduced here. For the working fluid in single phase state, i.e., the fluid in the sub-cooling zone (point 1 to point 2) and in the sup-heating zone (point 3 to point 4, point 5 to point 6), heat transfer coefficients (α_f) can be calculated using the correlation as follows [4,34]. It is a practically useful semi-empirical equation for heat transfer in technical plates based on the Leveque analogy and on experimental evidence:

$$\mathrm{Re} = \rho \cdot v \cdot D_{eq} / \mu \tag{10}$$

$$\mathrm{Pr} = cp \cdot \mu / k \tag{11}$$

$$1/f^{0.5} = \cos\beta/(0.18 \cdot \tan\beta + 0.36 \cdot \sin\beta + f_0/\cos\beta)^{0.5} + (1 - \cos\beta)/(3.8 \cdot f_1)^{0.5} \tag{12}$$

When $\mathrm{Re} < 2000$, $f_0 = 64/\mathrm{Re}$, $f_1 = 579/\mathrm{Re} + 3.85$
When $\mathrm{Re} \geqq 2000$, $f_0 = (1.8 \cdot \lg \mathrm{Re} - 1.5)^{-2}$, $f_1 = 39/\mathrm{Re}^{0.289}$

$$\mathrm{Nu} = 0.122 \cdot \mathrm{Pr}^{1/3} \cdot (\mu/\mu_{wall})^{1/6} (f \cdot \mathrm{Re}^2 \cdot \sin 2\beta)^{0.374} \tag{13}$$

$$\alpha = \mathrm{Nu} \cdot k / D_{eq} \tag{14}$$

Wherein, D_{eq} in Eq. (10) should be the equivalent diameter of working fluid channel.

$$D_{eq} = 2b/\varphi \tag{15}$$

b is corrugation depth and φ is the surface enlargement factor of a plate heat exchanger.

The cooling water side HTC (α_{cw}) is evaluated by the same model as that of single-phase working fluid above [34].

The Cooper's pool boiling correlation is chosen for HTC (α_e) calculation of the working fluid evaporating process (point 2 to point 3).

$$\alpha_e = 1.5 * 55 \cdot (p_e/p_{cr})^{(0.12 - 0.2 \cdot \lg Rp)} \cdot (-1g(p_e/p_{cr}))^{-0.55} \cdot q^{0.67} \cdot M^{-0.5} \tag{16}$$

Wherein, p_{cr} means the critical pressure of working fluid (MPa); R_p means the mean asperity height (μm), which is the mean roughness between peak and valley at surface. According to the supplied plate type heat exchangers by a European company, the value of R_p is 0.3 in this calculation; q means the heat flux (W/m^2), which is evaluated by assuming initial wall temperature, and then using the iterative method; M means the molar mass of working fluid (kg/kmol).

In condenser, the condensation heat transfer coefficient (α_c) of all working fluid can be calculated using the correlation as follows [35].

$$\alpha_l = 0.2092 * (k_l/D_{eq}) \cdot \mathrm{Re}_l^{0.78} \cdot \mathrm{Pr}_l^{0.33} \cdot (\mu/\mu_{wall})^{0.14} \quad (17)$$

$$\mathrm{Re}_l = G \cdot D_{eq}/\mu_l \quad (18)$$

$$\mathrm{Pr}_l = cp_l \cdot \mu_l/k_l \quad (19)$$

$$\mathrm{Co} = (\rho_v/\rho_l) \cdot (1/x - 1)^{0.8} \quad (20)$$

$$\mathrm{Fr}_l = G^2/(\rho_l^2 \cdot g \cdot D_{eq}) \quad (21)$$

$$\mathrm{Bo} = q/G \cdot i_{fg} \quad (22)$$

$$\alpha = \alpha_l \cdot (0.25 \cdot \mathrm{Co}^{-0.45} \cdot \mathrm{Fr}_l^{0.25} + 75 \cdot \mathrm{Bo}^{0.75}) \quad (23)$$

Wherein, x means vapor quality; G means mass flux of the working fluid (kg/m^2 s); g means the acceleration due to gravity (m/s^2); i_{fg} means the enthalpy of vaporization (kJ/kg).

Correlations chosen for transcritical systems (Fig. 4) are mostly the same as those of the subcritical systems, except the heating process of working fluid (point 1 to point 4). During this process, the Jackson correlation below is used to calculate the HTC (α_{hsf}). The Jackson correlation was regarded as one of the most accurate correlations since 97% of experimental data were correlated with the accuracy of ±25% [36].

$$\mathrm{Nu} = 0.0183 \cdot \mathrm{Re}^{0.82} \cdot \mathrm{Pr}^{0.5} \cdot (\rho_{wall}/\rho)^{0.3} \cdot (\overline{cp}/cp)^n \quad (24)$$

$$\begin{array}{ll} n = 0.4, T < T_w < T_{pc}, & 1.2 * T_{pc} < T < T_w \\ n = 0.4 + 0.2 * [(T_w/T_{pc}) - 1], & T < T_{pc} < T_w \\ n = 0.4 + 0.2 * [(T_w/T_{pc}) - 1] * [1 - 5 * (T/T_{pc} - 1)], & T_{pc} < T < 1.2 * T_{pc}, T < T_w \end{array}$$

Calculations of α, Re and Pr are the same as Eqs. (10) and (11). Besides, ρ_{wall} is the density of the working fluid of the wall-temperature. $\overline{cp}$ is the averaged over cross-section specific heat under constant pressure, $\overline{cp} = (h_w - h)/(T_w - T)$

Step 3, calculate total heat transfer coefficient (tHTC). Based on the HTCs of each side calculated above and the heat conductivities of heat exchanger materials, tHTC (K) can be calculated as,

$$1/K = 1000/\alpha_{hot\text{-}side} + t/\lambda + 1000/\alpha_{cold\text{-}side} \quad (25)$$

Step 4, the capacity of a heat exchanger, namely, the heat transfer area, is obtained as

$$A = Q/K/\Delta T_m \quad (26)$$

In addition, heat transfer area per net power A_s is an index reflecting the system's compactness. It influences the system's economic performance to some extent [37].

$$A_s = A/P_{net} \quad (27)$$

3.4.2. Investment calculations

Knowing the capacity of each component of an ORC system, investment modeling is conducted in three steps below [30]:

Step 1, calculations of ORC capital cost.

The capital cost of an integrated chemical plant takes into consideration many costs other than the purchased cost of the equipment. Factors associated with capital cost includes direct project expenses (such as equipment free-on-board cost, material required for installation and labor to install the system), indirect project expenses (such as freight, insurance, taxes, construction overhead and contractor engineering expenses), contingency and contractor fee, and auxiliary facilities (such as site development, auxiliary building, off-sites and utilities). In addition, the material factors and pressure factors are taken into account in the cost evaluation. The investment model of each component as well as coefficients referred is listed in Table 2 referring to [30]. The coefficients are selected based on the above capacity evaluation of each component. Besides, the components' types are required in order to choose proper coefficients from the data base in [30] which was obtained from a survey of equipment manufacturers. Therefore, the coefficients listed in Table 2 are mainly chosen for the two case studies in Section 4 (MA-ES Applications).

The capital cost based on economic situation in year 2012 is obtained below,

$$Cost_{2001} = C_{bm,\exp} + C_{bm,fp} + C_{bm,preh} + C_{bm,e} + C_{bm,suph} + C_{bm,c} \quad (28)$$

$$Cost_{2012} = Cost_{2001} \cdot CEPCI_{2012}/CEPCI_{2001} \quad (29)$$

Wherein, CEPCI_{2001} = 397, CEPCI_{2012} = 584.6 (CEPCI means Chemical Engineering Plant Cost Index).Step 2, calculation of annual investment on ORC.Capital recovery factor (CRF) is estimated based on the following equation.

$$CRF = i \cdot (1 + i)^{time}/((1 + i)^{time} - 1) \quad (30)$$

The annuity of the investment A_{nk} can be obtained using equation

$$A_{nk} = Cost_{2012} \cdot CRF \quad (31)$$

i is interest rate, whose value is 5%; *time* is economic life time, whose value is 15 years [20];

Step 3, EPC calculation. Electricity production cost (EPC) can be obtained by equation

$$EPC = (A_{nk} + f_K \cdot Cost_{2012})/((P_{\exp} - P_{fp}) \cdot h_{full\text{-}load}) \quad (32)$$

f_K is operation, maintenance and insurance cost factor, whose value is 1.65%; $h_{full\text{-}load}$ is full-load operation hours, whose value is 7500 h.

Step 4, DPP calculation. The depreciated payback period (DPP) is the number of time periods (years) that are required to recover the initial investment with all cash flows discounted back to the start-up year [40,41]. It is given by

$$DPP = -\ln(1 - k \cdot Cost_{2012}/F_{n0})/\ln(1 + k) \quad (33)$$

$$F_{n0} = \mathrm{E}_P \cdot ((P_{\exp} - P_{fp}) \cdot h_{full\text{-}load}) - f_K \cdot Cost_{2012} \quad (34)$$

The discount rate k is 5% in this text; $Cost_{2012}$ is the initial investment; F_{n0} is the net cash flow for year n without considering the inflation rate and is assumed to remain constant during the lifetime. In an ORC system, the net cash flow F_{n0} is the difference value between benefit and cost annually. The benefit specifically represents the revenue from selling produced electricity at a price of 0.2$/kW h, and the annual cost refers to the operation, maintenance and insurance cost which is set as $f_K \cdot Cost_{2012}$ according to Eq. (32).

Step 5, NPV calculation. The net present value (NPV) is another frequently-used economic index that sums the discounted cash flows of an energy system. It integrates and converts at the same time amounts of money of various time periods [42]. It is given by

$$NPV = -Cost_{2012} + \sum_{n=1}^{N} F_n/(1 + k)^n \quad (35)$$

$$F_n = F_{no} \cdot (1 + \mathrm{r})^n \quad (36)$$

n is the time period (year); N is the number of years for which the economic evaluation is requested; F_n is the net cash flow for year n considering the inflation rate r (2%). A project investment should be realized only if NPV > 0, and the best project should be the one with the highest NPV. It provides a basic criterion for economic evaluation.

Table 2
Investment models used in Way3 evaluations of MA-ES.

Components	Base module cost models	Coefficients				
		$K_1/K_2/K_3$	$C_1/C_2/C_3$	B_1/B_2	F_M	F_{bm}
Expander	$C_{bm,expander} = C_{p,e}F_{bm,e}$ $\lg C_{p,e} = K_{1,e} + K_{2,e}\lg P_e + K_{3,e}(\lg P_e)^2$	$K_1 = 2.705$ $K_2 = 1.440$ $K_3 = -0.177$	/	/	/	6.2
Pump	$C_{bm,pump} = C_{p,pump}F_{bm,pump}$ $\lg C_{p,pump} = K_{1,p} + K_{2,p}\lg P_p + K_{3,p}(\lg P_p)^2$ $F_{bm,pump} = B_{1,p} + B_{2,p}\cdot F_{M,pump}\cdot F_{P,pump}$ $\lg F_{P,pump} = C_{1,p} + C_{2,p}\lg P_P + C_{3,p}(\lg P_P)^2$	$K_1 = 3.870$ $K_2 = 0.316$ $K_3 = 0.122$	$C_1 = -0.245$ $C_2 = 0.259$ $C_3 = -0.014$	$B_1 = 1.89$ $B_2 = 1.35$	2.35	/
Evaporator/heater	$C_{bm,heater} = C_{p,heater}F_{bm,heater}$ $\lg C_{p,heater} = K_{1,h} + K_{2,h}\lg A_h + K_{3,h}(\lg A_h)^2$ $F_{bm,heater} = B_{1,h} + B_{2,h}\cdot F_{M,heater}$	$K_1 = 4.666$ $K_2 = -0.156$ $K_3 = 0.155$	/	$B_1 = 0.96$ $B_2 = 1.21$	2.45	/
Condenser	$C_{bm,condens} = C_{p,condens}F_{bm,condens}$ $\lg C_{p,condens} = K_{1,c} + K_{2,c}\lg A_c + K_{3,c}(\lg A_c)^2$ $F_{bm,condens} = B_{1,c} + B_{2,c}\cdot F_{M,condens}$	$K_1 = 4.666$ $K_2 = -0.156$ $K_3 = 0.155$	/	$B_1 = 0.96$ $B_2 = 1.21$	2.45	/

Other useful economic indexes could be extended based on capital investment above in this section in order to investigate more detailed economic performance from different perspectives [30].

3.5. MA-ES evaluation procedure

Summing from Sections 3.1 to 3.4, the MA-ES evaluation procedure is basically shown in the flow diagram of Fig. 5. This procedure clearly reflects the methodology of the MA-ES with ORC performance calculations and optimizations. Besides, the principle in this procedure is applicable to other ORC modifications by adjusting specific parameters correspondingly using MA-ES.

4. MA-ES applications

4.1. Case Study A: Evaluations and comparisons of ORC working fluids and operation modes

In this case, a bottoming ORC system is constructed to recover waste heat of exhaust gas released from a heavy-duty diesel engine. In a typical diesel engine, more than one third energy of the engine fuel is lost through exhaust gas, so it is of great economic and environmental importance to recover waste heat from the exhaust [38,39]. The bottoming ORC system configuration is the same as shown in Fig. 2 above, including two heat exchangers for vapor generation and condensation respectively, a pump and an expander. The subcritical and transcritical systems are both investigated with T–S figures just the same as Figs. 3 and 4. Four working fluids are selected for their good performance as explored in the previous work [4], which are R123, R245fa, R134a and R32. Their thermodynamic properties can be obtained from the database of the software Engineering Equation Solver (EES). The MA-ES built above is applied in this case for practical use.

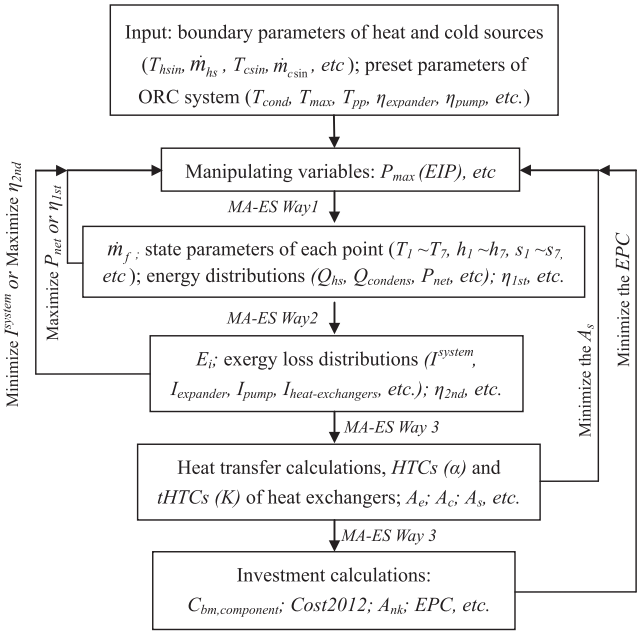

Fig. 5. MA-ES modeling flow diagram.

4.1.1. System settings of Case A

In addition to basic system assumptions made above, more assumptions as well as boundary conditions are required to be clarified for the given application. The heat source studied in this case is diesel exhaust under the rated condition. The composition of the exhaust gas on mass basis has been calculated as: CO_2 = 15.1%, H_2O = 5.5%, N_2 = 71.6%, O_2 = 7.8%. This composition is used to evaluate gas properties. Detailed parameters setting for system operation are listed in Table 3. Besides, structure dimensions of heat exchangers that derived from series products are listed in Table 4. The EIP of the working fluid is selected as the manipulated variable. In subcritical cycles, it is increased from the pressure slightly higher than the condensing pressure to the pressure closing to the critical point. In transcritical cycles, it is increased from pressure slightly above the critical point to 10 MPa.

4.1.2. Evaluation results of Case A

Evaluation results about six main indexes of Case Study A are summarized and compared in Figs. 6 and 7. Moreover, Appendix A complements important results of this case study for further understanding about the evaluation process. Appendix A comprises calculation parameters of four fluids under both subcritical and transcritical modes, including mass flow rate ($\dot{m}_f$), enthalpy values of key points (h_1–h_7), work capacity of key equipments (P_{exp}, P_{fp}), energy absorbed from heat source (q_a), system exergy loss (I^{system}), exergy loss ratios of components ($RatioI_{vg}$, $RatioI_{exp}$, $RatioI_{fp}$, $RatioI_{cond}$ and $RatioI_{cout}$), heat transfer coefficients (K), heat transfer areas (A) and the annuity of the investment (A_{nk}). Parameters of operations with EIP of 3 MPa and 10 MPa are chosen to represent subcritical and transcritical performance separately. Combining Figs. 6 and 7 and Appendix A, the evaluation results of Case Study A can be concluded as follows.

Table 3
Boundary conditions of Case Study A.

Parameters	Values	Parameters	Values
Hot source: exhaust temperature [K]	792.15	Expander efficiency [/]	0.7
Hot source: exhaust pressure [MPa]	0.12	Pump efficiency [/]	0.8
Hot source: exhaust mass flow [kg/s]	0.29	Condensing temperature [K]	308
Cold source: water temperature [K]	298.15	Expander inlet temperature EIT [K]	500
Cold source: water mass flow [kg/s]	4	Ambient temperature (dead state) [K]	298.15
TDPP [K]	30	Ambient pressure (dead state) [MPa]	0.101

Table 4
Main geometric dimensions of plate heat exchangers.

Parameters	Values
Chevron angle, β [degree]	60
Surface enlargement factor, φ [/]	1.117
Plate width, *Lw* [m]	0.119
Plate thickness, *t* [m]	0.0003
Mean asperity height, *Rp* [μm]	0.3
Corrugation depth, *b* [m]	0.00224
Equivalent diameter of liquid side, *Deq* [m]	0.004
Equivalent diameter of gas side, *Deqg* [m]	0.009
Coefficient of thermal conductivity, λ [kW/(m K)]	0.00163

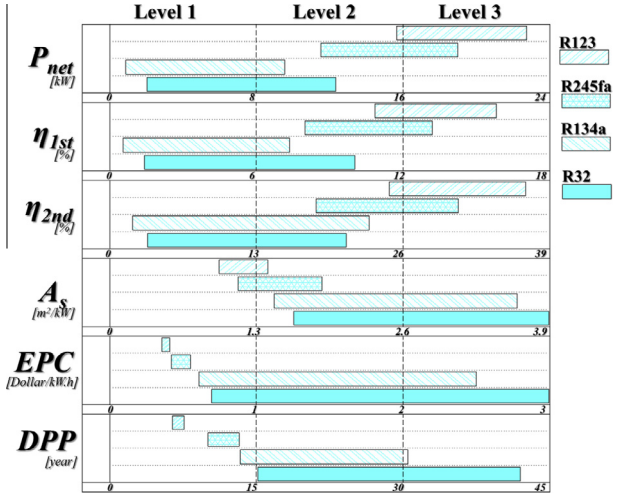

Fig. 6. Evaluations of subcritical ORC systems of Case Study A.

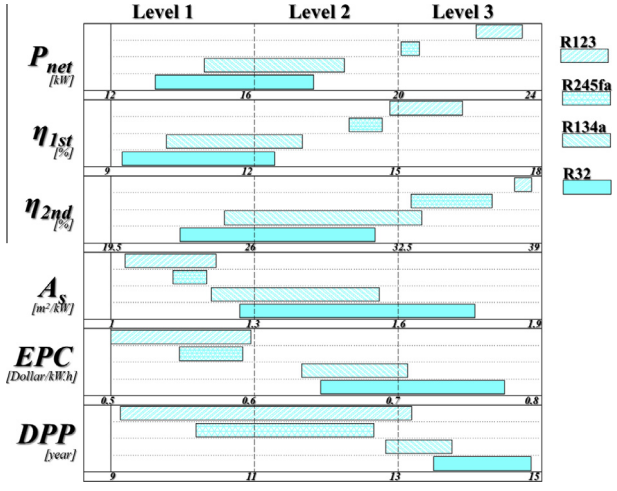

Fig. 7. Evaluations of transcritical ORC systems of Case Study A.

The results are graded into three levels by comparing the performance of four working fluids so as to clearly compare their relative merits. In subcritical operations shown in Fig. 6, R123 and R245fa gain clearly better performance based on the 1st law of thermodynamics analysis, with higher net power output and system efficiency ranking across Level 2 to Level 3. These advantages are more obvious in transcritical operations as shown in the first two rows of Fig. 7.

Similarly, the exergy efficiency of R123 is much higher than those of the remaining fluids under both subcritical and transcritical conditions. It is ranked the highest in Level 3, with maximal value of 38.5% with EIP of 10 MPa. The R245fa gets the second best performance of exergy efficiency. Moreover, the exergy is mainly lost during the heat transfer between the exhaust gas and the working fluid, as shown in Appendix A, and similar results were proved by other scholars [29]. Under subcritical conditions, the second greatest exergy loss occurs in condensation process during the heat transfer between the working fluid and the cooling water. However, the exergy loss in the expansion process exceeds that of condensation process when the EIP increases from subcritical pressure to transcritical pressure.

The evaluations of heat transfer areas per net power A_s are shown in the fourth rows in Figs. 6 and 7. Smaller A_s means less volume and weight of the system and better compactness. Besides, since heat exchangers are key components of an ORC system, smaller heat areas are beneficial to system cost if manufacturing complexity is ignored. As revealed in Fig. 6 and 7, A_s of four fluids show more or less the opposite trends to the first three indexes. Namely, the A_s values of R123 and R245fa are all at very low level under both subcritical and transcritical modes. The first reason is that they get more net power as shown in the first rows. The second reason is that system heat is transferred more efficiently with higher transfer coefficients, as shown in Appendix A. According to Eq. (27), the areas per power are thus apparently lower.

The electricity production costs (EPC) of R123 and R245fa are much lower than those of the other two working fluids in both subcritical and transcritical operation modes. They are all ranked at Level 1 that represents a better economic level. However, the annuities of the investments (A_{nk}) of R123 and R245fa, which represent system investments, are higher than those of the other two working fluids, as indicated in Appendix A. According to Eq. (32), the low electricity production costs are result from high net power.

According to the DPP comparison in the last row of Fig. 6, R123 reveals the absolutely best economic performance since it requires the shortest payback time which ranges from 6.4 to 7.6 years. Besides, the system needs 10.1–13.3 years to recover the initial investment applying R245fa. It is actually a quite long period for a real project but it is still a first-level-ranking one comparing to that applying R134a and R32. Additionally, the NPV in Appendix A further reveals the economic validity of each kind of fluid in subcritical mode. According to the NPV definition, the project could not be economically realized applying R32 when EIP is 3 MPa, and R123 is proved to be the best one with the highest NPV.

However, the economic performance of R134a and R32 improves great when the system turns to transcritical mode.

Besides of the obviously decreased EPCs, their DPPs decrease greatly from 15–45 years level to 13–15 years level. It could be explained by the increasing net power and the decreasing specific area which together reduce the investment and raise the benefits. However, the high EIP in transcritical mode does not obviously benefit the investment recovery for R123 and R245fa. The reason is that for these two fluids, the benefits brought by the increasing new power and decreasing specific area do not exceed much the costs brought by the bigger capacities of the expander and pump which result in higher investment. However looking from the NPV perspective, all four systems could be economically realized under transcritical pressure of 10 MPa, and R245fa and R123 are proved to be better alternatives wither higher NPV.

In conclusion, four conventional different working fluids and two typical operation modes are evaluated and compared in this case study applying the proposed MA-ES. R123 and R245fa are evaluated as the most appropriate working fluids for this application with excellent performance in three aspects of ORC system. In addition, it can be concluded by comparing the two result figures (Figs. 6 and 7) and data in Appendix A that, performance of transcritical cycle is mostly better than that of subcritical cycle for a certain fluid under the given heat source condition. However, it should be noted that if the subcritical and transcritial modes need to be investigated in practical applications, a single map could be much clearer with the same scale by combining Figs. 6 and 7.

4.2. Case Study B: Evaluations and comparisons of ORC configurations

In a typical diesel engine, less than 45% of fuel energy might be converted into useful work output from crankshaft, and the remaining energy is mainly lost through exhaust gas and jacket water. However, the energy in the two heat sources differs greatly in temperature regime, namely, the energy quality. The temperature of exhaust gas is about 500–800 K, while that of jacket water is below 400 K. Two configurations of bottoming ORC system – Single loop ORC and Dual loop ORC – have been explored for heat recovery from both heat sources. Single loop ORC systems were discussed in Refs. [8,29] using jacket water to preheat working fluid before being evaporated by exhaust gas. Dual-loop ORC systems were researched in Refs. [10,25,26,28]. Waste heat from two heat sources were recovered using cascade loops according to their temperature gradients. The two ORC strategies showed respective advantages in engine applications by assessing only a few performance indexes. In this case, their comprehensive performance can be assessed and compared applying the proposed evaluation system to further demonstrate the application values of the MA-ES.

In this case, two bottoming ORC systems, a single-loop (SL) ORC and a dual-loop (DL) ORC, are constructed to recover waste heat from both exhaust gas and jacket water released from the same heavy-duty diesel engine as used in Case A. Figs. 8 and 9 show the schematic diagrams the two ORC systems proposed. In the single-loop ORC system, working fluid is firstly preheated by jacket water and then evaporated and superheated by exhaust gas within a single ORC circuit, as shown in Fig. 8. The dual-loop ORC system contains a high-temperature loop (HL) ORC and a low-temperature loop (LL) ORC, as shown in Fig. 9. The HL ORC is designed to recover the high-temperature part of exhaust waste heat, which guarantees the system's safety. The LL ORC is designed to recover the engine waste heat in jacket water, residual heat from the HL ORC during its condensation process and low-temperature part of the exhaust waste heat successively.

4.2.1. System settings of Case B

Boundary conditions in this case study such as ambient conditions, exhaust gas conditions and heat exchangers' structures are the same as in Case A. Additional settings for the two ORC operations in this case are listed in Table 5. In the single-loop (SL) ORC system, R245fa is adopted as the working fluid for its excellent performance revealed in Case Study A. The subcritical and transcritical operations are both considered based on this ORC configuration. In subcritical cycles, EIP is increased from 1 MPa to the pressure closing to the critical point. In transcritical cycles, EIP is increased from the pressure slightly above the critical point to 10 MPa. In the dual-loop (DL) ORC system, water and R245fa are adopted as the working fluid for high loop and low loop respectively based on investigations of fluids screening [25]. Both loops are supposed to be operated under subcritical pressures. EIP of the high loop increases from 1 MPa to 6 MPa, since the pressures above 6 MPa will result that the working vapor after expansion falls into two-phase region. EIP of low loop is set at 0.58 MPa.

4.2.2. Evaluation results of Case B

Evaluation results about five main indexes of Case Study B are summarized and compared in Fig. 10. Appendix B complements key results of this case study. Overall, the performance of the transcritical cycle is much better than that of the subcritical one considering only the Way1 and Way2 evaluations when single-loop ORC system is adopted. These regularities are quite similar to those explained in Case Study A. However, the dual-loop system changes the performance dramatically as summarized as follows.

Firstly, the dual-loop system can gain more than twice the net power of single-loop systems. Total net power of two cascade loops is within 35–38 kW range under the pressure concerned. This is quite meaningful for internal combustion engines that are stuck in the bottleneck period of power and efficiency lifting. As for system efficiency η_{1st}, it is ranked at mid-high level of the dual-loop system comparing to that of the single-loop system. However, the dual-loop system shows no obvious advantage in the efficiency performance over the single loop systems, especially the transcritical one. Besides, the system efficiency does not increase greatly as the EIP of high loop increases. It only changes within a small range about 11.5–13% when the high loop EIP increases from 1 MPa to 6 MPa. After all, the dual-loop system performs well enough in the Way1 evaluation part.

Exergy efficiency is another great advantage of the dual-loop system with a high value range of 42.1–45.0%, which is right over that of the single-loop system. Total exergy losses of the whole dual-loop ORC system is roughly twice of that of the single-loop system, as shown in Appendix B. Higher exergy loss in the dual-loop system are mainly resulted from larger amount of component needed in the cycle. But higher exergy efficiencies reveal that the waste energy is more efficiently utilized in the dual-loop ORC system.

The A_s value range of dual-loop system is similar to that of the transcritical single-loop system. Both of them are ranked at the mid-high levels, which are higher than that of the subcritical single-loop system.

Although the amount of the component's in dual-loop system is definitely larger than that of the single-loop system, its electricity production costs (EPC) are much lower with a range of about 0.67–0.73 Dollar/kW h.

The biggest advantage of the SL-Subcritical system is the shortest depreciated payback time (DPP) it needs. According to the last row of economic index comparison in Fig. 10, only about 2.8–4.5 years are needed under the given pressures using SL-Subcritical configuration. Although the net power output is the lowest of this system configuration comparing to those of the other two, the components' capacities in this system are much lower, leading to the least initial investment and the shortest payback time.

On the contrary, the SL-Transcritical system requires the longest payback time which is within 18.7–22.2 years, while the DL

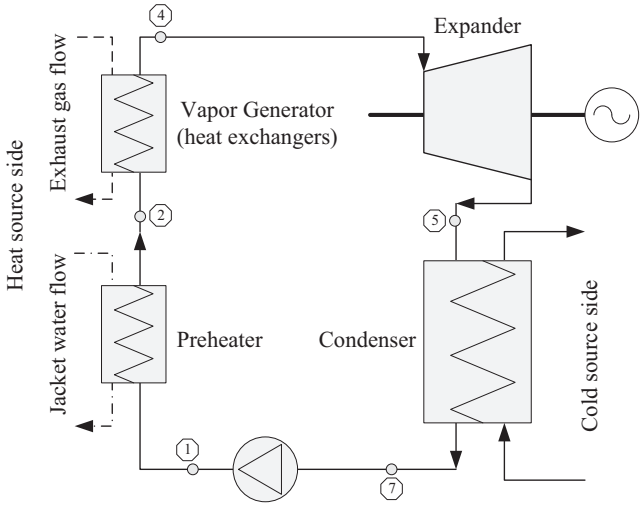

Fig. 8. Schematic diagram of the single-loop (SL) ORC system of Case Study B.

system shows moderate performance concerning the DPP comparison. Generally the DPP index separates the three configurations obviously by ranking them into different levels. In addition, according to Appendix B, NPV values of the SL-Transcritical system are both negative under the two pressures selected, proving that they could not be economically realized in these situations. The SL-Subcritical and DL systems are proven to be valid to some extent with high NPVs.

Another meaningful index is the heat recovery amount, as shown in Appendix B. It shows that, two ORC configurations proposed in this case study are able to recover almost equal amount of waste energy from the exhaust gas source (Q_g). But the dual-loop system is much more efficient in recovering waste energy from the jacket water source (Q_{jw}). Its recovery amount is ten times more than that of the single-loop system.

In conclusion, three ORC configurations are evaluated and compared in this case study applying the proposed MA-ES. The dual-loop ORC system is evaluated as a relatively proper configuration for waste heat recovery in this case study. It performs excellently during Way1 and Way2 evaluations with high thermodynamic indexes, while its economic performance is not much outstanding

Table 5
Boundary conditions of Case Study B.

Parameters	Values
Temperature of inlet jacket water [K]	356.5
Pressure of inlet jacket water [MPa]	0.12
Mass flow of inlet jacket water [kg/s]	2.7
Difference between EIT and inlet exhaust temperature [K]	40
TDPP between exhaust gas and working fluid [K]	30
TDPP between jacket water and working fluid [K]	5
Condensing temperature of single-loop ORC [K]	310
Condensing temperature of double-loop ORC [K]	348/310

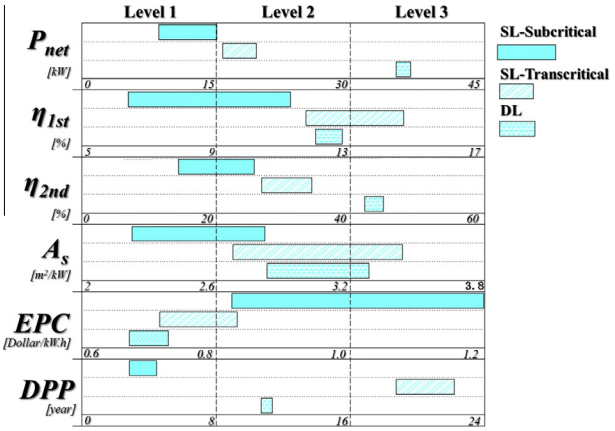

Fig. 10. Evaluations of ORC systems of Case Study B.

compared to single-loop systems. So more optimizations are needed and investors should weigh up all indexes to make the decision.

5. Conclusions

A comprehensive evaluation system of ORC performance (MA-ES) is established, which provides a general method of ORC performance assessment, without restrictions to system configurations, operation modes, applications, working fluid types, equipment

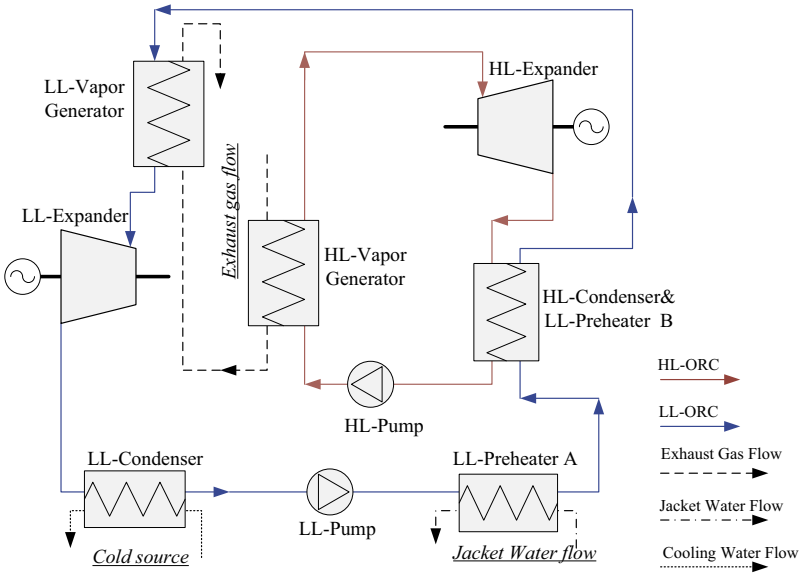

Fig. 9. Schematic diagram of the dual-loop (DL) ORC system of Case Study B.

conditions and process parameters, etc. The evaluation system covers three main aspects of typical ORC performance: basic thermodynamic evaluations based on the 1st law of thermodynamics and the 2nd law of thermodynamics, economic evaluations based on calculations of equipment capacity, investment and cost recovery. The evaluations will provide valuable guidance for ORC design, equipment selection and system construction.

Two typical ORC cases of engine waste-heat-recovery are investigated in this work to illustrate the applications of the MA-ES. Under the first case condition, the performance of the transcritical cycle is much better than that of subcritical cycle for a certain fluid. And comparing with other two common fluids, R123 and R245fa are evaluated as more appropriate working fluids for this application with excellent performance in three aspects of ORC system. Under the second case condition, the dual-loop ORC system is a relatively proper configuration for waste heat recovery, which performs excellently during thermodynamic evaluating processes and shows moderate performance in economic evaluations.

Acknowledgment

This work was sponsored by the National Natural Science Foundation of China (No. 51206117).

Appendix A

Evaluation results of Case Study A.

	Units	Subcritical ORC (p_{max} = 3 MPa)				Supercritical ORC (p_{max} = 10 MPa)			
		R32	R134a	R245fa	R123	R32	R134a	R245fa	R123
$\dot{m}_f$	kg/s	0.302	0.397	0.391	0.476	0.344	0.468	0.506	0.669
h_1	kJ/kg	266.1	102.9	248.3	239	275.5	110.3	255	245
h_2	kJ/kg	293	186.5	417.4	404.8	/	/	/	/
h_3	kJ/kg	508.5	279.1	488.8	468.7	/	/	/	/
h_4	kJ/kg	743.1	465.1	615.9	541.5	688.6	414.6	537.2	458.4
h_5	kJ/kg	726.5	433.9	566.7	492.5	626.8	365.4	487.3	418.2
h_6	kJ/kg	514.5	269	430	404	514.5	269	430	404
h_7	kJ/kg	265	100.7	245.6	236.5	265	100.7	245.7	236.5
P_{exp}	kW	4.99	12.36	19.25	23.27	21.26	23	25.27	26.89
P_{fp}	kW	0.336	0.896	1.038	1.186	3.607	4.49	4.684	5.712
Q_g	kW	144.1	143.8	143.9	143.9	142.1	142.4	142.9	142.8
I^{system}	kW	59.55	52.71	45.97	42.1	46.33	45.51	43.49	42.89
$RatioI_{gf}$	%	69.47	61.9	59.11	57.79	65.6	60.81	62.69	62.37
$RatioI_{exp}$	%	2.235	6.55	12.42	17.13	15.28	16.52	20.92	25.25
$RatioI_{fp}$	%	0.109	0.323	0.435	0.541	1.474	1.874	2.057	2.533
$RatioI_{cond}$	%	25	27.98	24.68	21.09	14.38	17.5	10.97	6.465
$RationI_{cout}$	%	3.186	3.247	3.36	3.446	3.27	3.298	3.364	3.374
K_{gf}	kW/(m^2 K)	/	/	/	/	0.090	0.089	0.086	0.0854
K_{gf_pre}	kW/(m^2 K)	0.085	0.085	0.096	0.097	/	/	/	/
K_{gf_evp}	kW/(m^2 K)	0.107	0.110	0.116	0.119	/	/	/	/
K_{gf_suph}	kW/(m^2 K)	0.109	0.110	0.114	0.114	/	/	/	/
K_{fcw_cond}	kW/(m^2 K)	1.561	1.376	1.373	1.588	1.658	1.513	1.64	1.969
K_{fcw_supc}	kW/(m^2 K)	0.810	0.858	0.8892	0.753	0.8456	0.9104	0.9551	0.5115
A_c	m^2	8.164	7.975	8.493	8.531	8.989	8.776	9.93	11.57
A_e	m^2	10.24	12.62	13.24	13.77	13.43	13.71	14.21	14.26
A_{nk}	Dollar	52,910	60,821	66,985	70,479	73,059	75,299	78,046	81,092
NPV	Dollar	−84,032	24,582	147,710	309,068	66,430	64,857	98,865	88,035

Appendix B

Evaluation results of Case Study B.

	Single-loop sub-ORC				Single-loop sup-ORC			Double-loop ORC					
	Units	P_{max}	2 MPa	3 MPa	6 MPa	8 MPa		Units	2 MPa	4 MPa	Units	2 MPa	4 MPa
$\dot{m}_f$	kg/s	0.186	0.188	0.1891	0.1903	$\dot{m}_{f1}$	kg/s	0.03435	0.032	$ratioI_{cout}$	%	8.816	8.884
h_1	kJ/kg	250.000	251.000	253.8	255.7	$\dot{m}_{f2}$	kg/s	1.185	1.181	$ratioI_{c2}$	%	15.080	15.282
h_2	kJ/kg	306.700	306.600	306.8	307	P_{exp1}	kW	21.450	22.270	$ratioI_{gf1}$	%	26.938	21.868

Appendix B (*continued*)

	Single-loop sub-ORC			Single-loop sup-ORC			Double-loop ORC					
	Units	P_{max}	2 MPa	3 MPa	6 MPa	8 MPa	Units	2 MPa	4 MPa	Units	2 MPa	4 MPa
h_3	kJ/kg	344.900	345.000	/	/	P_{exp2}	kW	15.230	15.170	$ratioI_{gf2}$	%	4.758	8.164
h_{3g}	kJ/kg	485.100	488.800	/	/	η_1	%	20.110	22.370	$ratioI_{pump1}$	%	0.031	0.060
h_4	kJ/kg	973.100	970.700	963.7	959.3	η_2	%	8.270	7.939	$ratioI_{pump2}$	%	0.163	0.165
h_5	kJ/kg	905.400	891.400	865.6	853.8	Q_{g1}	kW	106.700	99.540	$ratioI_{exp1}$	%	15.640	17.416
h_6	kJ/kg	431.500	431.500	431.5	431.5	Q_{g2}	kW	17.040	24.190	$ratioI_{exp2}$	%	12.418	12.559
h_7	kJ/kg	248.300	248.300	248.3	248.3	Q_{jw}	kW	167.100	166.900	$ratioI_{jwf2}$	%	11.274	11.426
P_{exp}	kW	12.610	14.860	18.56	20.08	h_1	kJ/kg	315.8	318.4	$ratioI_{f1f2}$	%	3.861	2.965
P_{fp}	kW	0.316	0.497	1.04	1.407	h_2	kJ/kg	908.7	1087	$HL\text{-}K_{gf1\_evp}$	kW/(m^2 K)	0.1137	0.1148
Q_g	kW	124.200	124.500	124.2	124.2	h_{2g}	kJ/kg	2799	2801	$HL\text{-}K_{gf1\_pre}$	kW/(m^2 K)	0.09875	0.09979
Q_{jw}	kW	10.560	10.440	10.02	9.769	h_3	kJ/kg	3421	3397	$HL\text{-}K_{gf1\_suph}$	kW/(m^2 K)	0.093	0.094
I^{system}	kW	48.180	46.150	43.19	41.76	h_4	kJ/kg	2794	2703	$LL\text{-}K_{supc2}$	kW/(m^2 K)	1.482	1.479
$ratioI_{cond}$	%	73.300	73.790	73.32	73.42	h_5	kJ/kg	313.3	313.3	$LL\text{-}K_{cond2}$	kW/(m^2 K)	2.736	2.731
$ratioI_{fp}$	%	0.126	0.206	0.522	0.679	h_{5s}	kJ/kg	2634	2634	$LL\text{-}K_{ff\_H}$	kW/(m^2 K)	0.1543	0.1463
$ratioI_{gf}$	%	18.330	16.490	13.7	12.80	h_6	kJ/kg	248.6	248.6	$LL\text{-}K_{ff\_L}$	kW/(m^2 K)	0.1694	0.161
$ratioI_{jwf}$	%	1.379	1.409	2.07	1.57	h_7	kJ/kg	389.7	390	$LL\text{-}K_{gf\_evp}$	kW/(m^2 K)	0.09163	0.0939
$ratioI_t$	%	4.827	6.039	8.32	9.44	h_{7s}	kJ/kg	456.9	453.6	$LL\text{-}K_{gf\_suph}$	kW/(m^2 K)	0.09692	0.09852
$rationI_{cout}$	%	2.040	2.065	2.09	2.092	h_8	kJ/kg	461.6	455.5	$LL\text{-}K_{jwf\_H}$	kW/(m^2 K)	1.909	1.909
K_{fcw_cond}	kW/(m^2 K)	0.840	0.843	1.042	1.046	h_9	kJ/kg	291.9	291.9	$LL\text{-}K_{jwf\_L}$	kW/(m^2 K)	1.359	1.356
K_{fcw_supc}	kW/(m^2 K)	0.734	0.731	0.7304	0.7284	h_{10}	kJ/kg	453.7	453.7	HL_A_e	m^2	11.010	10.690
K_{gf_evp}	kW/(m^2 K)	0.101	0.103	/	/	h_{11}	kJ/kg	476	476	LL_A_c	m^2	13.890	13.810
K_{gf_pre}	kW/(m^2 K)	0.085	0.086	/	/	h_{12}	kJ/kg	462.8	462.8	LL_A_{f1f2}	m^2	71.430	70.370
K_{gf_suph}	kW/(m^2 K)	0.103	0.103	/	/	h_{13}	kJ/kg	248.3	248.3	LL_A_{gf}	m^2	5.072	3.347
K_{gf}	kW/(m^2 K)	/	/	0.07338	0.07398	h_{13s}	kJ/kg	431.5	431.5	LL_A_{jwf}	m^2	9.240	9.234
K_{jwf}	kW/(m^2 K)	0.4963	0.4974	0.4983	0.4991	I^{system}	kW	84.16	84.19	A_{nk}	Dollar	162,800	161,800
A_c	m^2	4.765	4.773	4.09	4.097					*NPV*	Dollar	260,030	275,023
A_e	m^2	22.350	26.030	48.1	47.46								
A_{jwf}	m^2	1.176	1.169	1.146	1.132								
A_{nk}	Dollar	75,016	76,832	86,082	86,568								
NPV	Dollar	248,013	299,966	−44,953	−34,006								

References

[1] Lecompte S, Huisseune H, Broek MVD, Schampheleire SD, Paepe MD. Part load based thermo-economic optimization of the Organic Rankine Cycle (ORC) applied to a combined heat and power (CHP) system. Appl Energy 2013;111:871–81.

[2] Sylvain Q, Martijn VDB, Sebastien D, Pierre D. Techno-economic survey of Organic Rankine Cycle (ORC) systems. Renew Sustain Energy Rev 2013;22:168–86.

[3] Zhijun P, Tianyou W, Yongling H, Xiaoyi Y, Lipeng L. Analysis of environmental and economic benefits of integrated Exhaust Energy Recovery (EER) for vehicles. Appl Energy 2013;105:238–43.

[4] Hua T, Gequn S, Haiqiao W, Xingyu L, Lina L. Fluids and parameters optimization for the organic Rankine cycles (ORCs) used in exhaust heat recovery of Internal Combustion Engine (ICE). Energy 2012;47:125–36.

[5] Gequn S, Xiaoning L, Hua T, Xingyu L, Haiqiao W, Xu W. Alkanes as working fluids for high-temperature exhaust heat recovery of diesel engine using organic Rankine cycle. Appl Energy 2014;119:204–17.

[6] Qiang L, Yuanyuan D, Zhen Y. Effect of condensation temperature glide on the performance of organic Rankine cycles with zeotropic mixture working fluids. Appl Energy 2014;115:394–404.

[7] Daniele F, Giampaolo M, Francesco M. Thermo-fluid dynamics preliminary design of turbo-expanders for ORC cycles. Appl Energy 2012;97:601–8.

[8] Iacopo V, Agostino G. Internal Combustion Engine (ICE) bottoming with Organic Rankine Cycles (ORCs). Energy 2010;35:1084–93.

[9] Katsanos CO, Hountalas DT, Pariotis EG. Thermodynamic analysis of a Rankine cycle applied on a diesel truck engine using steam and organic medium. Energy Convers Manage 2012;60:68–76.

[10] Zhang HG, Wang EH, Fan BY. A performance analysis of a novel system of a dual loop bottoming organic Rankine cycle (ORC) with a light-duty diesel engine. Appl Energy 2013;102:1504–13.

[11] Lisa B, Andrea DP, Antonio P. Systematic comparison of ORC configurations by means of comprehensive performance indexes. Appl Therm Eng 2013;61:129–40.

[12] Huijuan C, Goswami DY, Rahman MM, Stefanakos EK. Energetic and exergetic analysis of CO2- and R32-based transcritical Rankine cycles for low-grade heat conversion. Appl Energy 2011;88:2802–8.

[13] Yiping D, Jiangfeng W, Lin G. Parametric optimization and comparative study of organic Rankine cycle (ORC) for low grade waste heat recovery. Energy Convers Manage 2009;50:576–82.

[14] Roy JP, Mishra MK, Misra A. Performance analysis of an Organic Rankine Cycle with superheating under different heat source temperature conditions. Appl Energy 2011;88:2995–3004.

[15] Tchanche BF, Lambrinos G, Frangoudakis A, Papadakis G. Exergy analysis of micro-organic Rankine power cycles for a small scale solar driven reverse osmosis desalination system. Appl Energy 2010;87:1295–306.

[16] Junjiang B, Li Z. Exergy analysis and parameter study on a novel auto-cascade Rankine cycle. Energy 2012;48:539–47.

[17] Qicheng C, Jinliang X, Hongxia C. A new design method for Organic Rankine Cycles with constraint of inlet and outlet heat carrier fluid temperatures coupling with the heat source. Appl Energy 2012;98:562–73.

[18] Jiangfeng W, Yiping D, Lin G. Exergy analyses and parametric optimizations for different cogeneration power plants in cement industry. Appl Energy 2009;86:941–8.

[19] Lecompte S, Huisseune H, Broek M, Schampheleire S, Paepe M. Part load based thermo-economic optimization of the Organic Rankine Cycle (ORC) applied to a combined heat and power (CHP) system. Appl Energy 2013;111:871–81.

[20] Schuster A, Karellas S, Kakaras E, Spliethoff H. Energetic and economic investigation of organic Rankine cycle applications. Appl Therm Eng 2009;29:1809–17.

[21] Shengjun Z, Huaixin W, Tao G. Performance comparison and parametric optimization of subcritical organic Rankine cycle (ORC) and transcritical power cycle system for low-temperature geothermal power generation. Appl Energy 2011;88:2740–54.

[22] Gewald D, Karellas S, Schuster A, Spliethoff H. Integrated system approach for increase of engine combined cycle efficiency. Energy Convers Manage 2012;60:36–44.

[23] Pedro JM, Rogelio L. Evaluation of the potential use of a combined micro-turbine organic Rankine cycle for different geographic locations. Appl Energy 2013;102:1324–33.

[24] Gequn S, Guopeng Y, Hua T, Haiqiao W, Xingyu L. Simulations of a bottoming organic rankine cycle (ORC) driven by waste heat in a diesel engine (DE). SAE 2013–01-0851.

[25] Gequn S, Lina L, Hua T, Haiqiao W, Youcai L. Analysis of regenerative dual-loop organic Rankine cycles (DORCs) used in engine waste heat recovery. Energy Convers Manage 2013;76:234–43.
[26] Ringler J, Seifert M, Guyotot V, Hübner W. Rankine cycle for waste heat recovery of IC engines. SAE 2009-1-0174; 2009.
[27] Daniel M, Javier R, Vincent L, Sylvain Q. Systematic optimization of subcritical and transcritical organic Rankine cycles (ORCs) constrained by technical parameters in multiple applications. Appl Energy 2014;117:11–29.
[28] Bo L, Philippe R, Christophe C, Renaud G, Franck D. Investigation of a two stage Rankine cycle for electric power plants. Appl Energy 2012;100:285–94.
[29] Guopeng Y, Gequn S, Hua T, Haiqiao W, Lina L. Simulation and thermodynamic analysis of a bottoming Organic Rankine Cycle (ORC) of diesel engine (DE). Energy 2013;51:281–90.
[30] Turton R, Bailie RC, Whiting WB, Shaeiwitz JA. Analysis, synthesis and design of chemical processes, 3rd ed.; 2008.
[31] Jianchang H, Sheer TJ, Michael B. Heat transfer and pressure drop in plate heat exchanger refrigerant evaporators. Int J Refrig 2012;35:325–35.
[32] Zahid HA. Plate heat exchanger literature survey and new heat transfer and pressure drop correlations for refrigerant evaporators. Heat Transfer Eng 2003;24:3–16.
[33] Kandylas IP, Stamatelos AM. Engine exhaust system design based on heat transfer computation. Energy Convers Manage 1999;40:1057–72.
[34] Martin H. A theoretical approach to predict the performance of chevron-type plate heat exchangers. Chem Eng Process 1996;35:301–10.
[35] Hsieh YY, Lie YM, Lin TF. Condensation heat transfer and pressure drop of refrigerant R-410a in a vertical plate heat exchanger. In: Third international symposium on two-phase flow modelling and experimentation, vol. 1, Pisa, Italy; 2004.
[36] Pioro IL, Khartabil HF, Romney BD. Heat transfer to supercritical fluids flowing in channels—empirical correlations (survey). Nucl Eng Des 2004;230:69–91.
[37] Hettiarachchi HDM, Golubovic M, Worek WM, Ikegami Y. Optimum design criteria for an organic Rankine cycle using low-temperature geothermal heat sources. Energy 2007;32:1698–706.
[38] Dolz V, Novella R, García A, Sánchez J. HD Diesel engine equipped with a bottoming Rankine cycle as a waste heat recovery system. Part 1: study and analysis of the waste heat energy. Appl Therm Eng 2012;36:269–78.
[39] Macián V, Serrano JR, Dolz V, Sánchez J. Methodology to design a bottoming Rankine cycle, as a waste energy recovering system in vehicles: study in a HDD engine. Appl Energy 2013;104:758–71.
[40] Bertrand FT. Low-grade heat conversion into power using small scale organic rankine cycles. Doctoral thesis. Agricultural University Of Athens; 2010.
[41] Yiannis N, Petros AP, Alexandros C. Economic evaluation of energy saving measures in a common type of Greek building. Appl Energy 2009;86:2550–9.
[42] Walter S, Daniel JP, Thomas H. Manual for the economic evaluation of energy efficiency and renewable energy technologies. National Renewable Energy Laboratory; March 1995.